Hepatic acute-phase proteins control innate immune responses during infection by promoting myeloid-derived suppressor cell function

Leif E. Sander,[1,2] Sara Dutton Sackett,[1] Uta Dierssen,[1] Naiara Beraza,[1] Reinhold P. Linke,[3] Michael Müller,[4] J. Magarian Blander,[2] Frank Tacke,[1] and Christian Trautwein[1]

[1]Department of Medicine III, RWTH University Hospital, 52074 Aachen, Germany
[2]Immunology Institute, Mount Sinai School of Medicine, New York, NY 10029
[3]Reference Center of Amyloid Diseases, 82152 Martinsried, Germany
[4]Nutrition, Metabolism, and Genomics Group, Division of Human Nutrition, Wageningen University, 6700 EV Wageningen, Netherlands

Acute-phase proteins (APPs) are an evolutionarily conserved family of proteins produced mainly in the liver in response to infection and inflammation. Despite vast pro- and anti-inflammatory properties ascribed to individual APPs, their collective function during infections remains poorly defined. Using a mouse model of polymicrobial sepsis, we show that abrogation of APP production by hepatocyte-specific gp130 deletion, the signaling receptor shared by IL-6 family cytokines, strongly increased mortality despite normal bacterial clearance. Hepatic gp130 signaling through STAT3 was required to control systemic inflammation. Notably, hepatic gp130–STAT3 activation was also essential for mobilization and tissue accumulation of myeloid-derived suppressor cells (MDSCs), a cell population mainly known for antiinflammatory properties in cancer. MDSCs were critical to regulate innate inflammation, and their adoptive transfer efficiently protected gp130-deficient mice from sepsis-associated mortality. The hepatic APPs serum amyloid A and Cxcl1/KC cooperatively promoted MDSC mobilization, accumulation, and survival, and reversed dysregulated inflammation and restored survival of gp130-deficient mice. Thus, gp130-dependent communication between the liver and MDSCs through APPs controls inflammatory responses during infection.

CORRESPONDENCE
Christian Trautwein:
ctrautwein@ukaachen.de
OR
Leif E. Sander:
leif.sander@mssm.edu

Abbreviations used: APP, acute-phase protein; CLP, cecal ligation and puncture; IL-1Ra, IL-1R antagonist; MAPK, mitogen-activated protein kinase; MDSC, myeloid-derived suppressor cell; SAA, serum amyloid A; TLR, Toll-like receptor.

Sepsis is a major cause of mortality worldwide characterized by a dysregulated inflammatory response to infection (Hotchkiss and Karl, 2003). Excessive inflammation accounts for serious complications, but unfortunately, strategies targeting key proinflammatory mediators have had only very limited success (Fisher et al., 1996; Riedemann et al., 2003), demonstrating the complex pathogenesis of the disorder that is determined by a variety of both pathogen and host factors. Notably, patients with chronic liver diseases have significantly increased risk of acquiring sepsis and its accompanying complications, and thus have higher sepsis-related mortality, with it accounting for 30% of all deaths in cirrhotic patients (Foreman et al., 2003). The underlying mechanisms for this clinical observation are only partially understood.

The liver is the major source of acute-phase proteins (APPs), which are defined as proteins whose serum levels change by >25% during inflammation (Gabay and Kushner, 1999), and they are regarded as important components of the innate immune response to infection (Medzhitov, 2007). Many APPs are known as potent opsonins (Shah et al., 2006) and activators of innate immune cells such as neutrophils (Cheng et al., 2008a), but they also have antiinflammatory properties (Zouki et al., 1997). Because of the large diversity of APPs with both pro- and antiinflammatory functions (Gabay and

Kushner, 1999), their overall role during infections is still not well defined.

IL-6 is widely viewed as the major inducer of APP production in hepatocytes (Ritchie and Fuller, 1983). However, APP production in IL-6–deficient mice is only partly impaired and varies depending on the stimulus (Kopf et al., 1994). This strongly suggests redundant functions of the IL-6 family cytokines, a large group of cytokines that share the common signaling receptor gp130 (Murakami et al., 1993), or compensatory APP induction by other cytokines such as TNF and IL-1β. Most IL-6 cytokines bind to a membrane-bound cognate receptor and form a signaling complex with two gp130 receptors. Phosphorylation of distinct tyrosines of the intracellular domains of gp130 leads to activation of STAT3 and/or Ras–mitogen-activated protein kinase (MAPK) signaling. To better define the function of the hepatic acute-phase response during sepsis and endotoxic shock, we investigated the role of gp130 and downstream intracellular signaling pathways in hepatocytes. Although local effects of hepatic gp130 deficiency have been well characterized (Klein et al., 2005), systemic consequences remain unknown.

Innate immune cell activation is critical for host defense against invading microorganisms and for the subsequent generation of an adaptive immune response (Medzhitov, 2007). On the other hand, proinflammatory mediators produced by innate immune cells are considered key elements in the pathogenesis of severe sepsis and multiorgan failure (Rittirsch et al., 2008). Tight control of proinflammatory pathways is therefore critical for immune homeostasis and host survival. A complex network of activating and regulatory pathways controls innate immune responses. In this study, we postulated that the hepatic acute-phase response crucially contributes to this regulation. Because one of the major proinflammatory mediators in sepsis, IL-6, is known to be a strong stimulator of APP production in the liver, we hypothesized that the resulting acute-phase response potentially acts as a counterregulator of the initial inflammatory reaction. We investigated whether hepatic APPs affect the central and peripheral immune cell composition, which undergoes dramatic changes during infections and endotoxemia. Interestingly, a growing body of evidence highlights the capacity of myeloid-derived suppressor cells (MDSCs), a heterogeneous, immature population of myeloid (precursor) cells characterized by the expression of the myeloid lineage marker Gr1 and CD11b, to inhibit T cell responses (Movahedi et al., 2008; Gabrilovich and Nagaraj, 2009). Although MDSCs are best known and characterized for their role in tumor immune evasion and promotion of metastasis (Nagaraj et al., 2007; Yang et al., 2008), they have also been associated with other pathological conditions like trauma, inflammation, and autoimmune disease (Zhu et al., 2007; Haile et al., 2008). Moreover, it has been reported that MDSCs accumulate in the spleens of mice during polymicrobial sepsis and suppress T cell functions (Delano et al., 2007). However, to which extent MDSCs modify the course of disease or if they critically contribute to immune regulation during sepsis remains unclear.

In the present study we find that gp130–STAT3 signaling in hepatocytes and subsequent APP production is required to control the inflammatory response by facilitating peripheral accumulation and survival of MDSCs in sepsis. We provide evidence that MDSCs can directly inhibit inflammatory immune responses and define them as a key autoregulatory component of the innate immune system during infection.

RESULTS

Hepatic gp130–STAT3 signaling protects against excessive inflammation during sepsis

To better define the role of the hepatic acute-phase response during systemic bacterial infections, we used the cecal ligation and puncture (CLP) model of polymicrobial sepsis (Buras et al., 2005). We had previously generated hepatocyte-specific gp130-deficient mice (*gp130Δhepa*), which carry loxP sites flanking exon 16 of the gp130 gene and express Cre recombinase under control of the albumin promoter (Betz et al., 1998; Streetz et al., 2003). We had further described hepatocyte-specific gp130 signaling–deficient mice, in which either gp130-induced STAT3 (*gp130StatΔhepa*) or Ras–MAPK (*gp130RasΔhepa*) signaling is impaired (Klein et al., 2005). The latter express knockin mutations in the intracellular domain of gp130 (Tebbutt et al., 2002) on one allele, whereas the other allele is floxed (Klein et al., 2005). *gp130RasΔhepa* mice selectively lack wild-type gp130 in hepatocytes expressing only the mutant *gp130^{757F}* allele in which the SHP-2 binding domain is mutated and subsequent SHP-2–Ras–extracellular signal-regulated kinase signaling is abrogated (Tebbutt et al., 2002; Klein et al., 2005). In *gp130StatΔhepa* mice, hepatocytes express a mutant gp130 allele with a truncated intracellular domain, thereby ablating STAT3 binding and phosphorylation (Ernst et al., 2001), whereas the second allele is deleted by Cre recombination (Klein et al., 2005). These mice allowed us to dissect the contribution of hepatic gp130–Ras–MAPK and gp130–STAT3 signaling, respectively, during sepsis. *gp130Δhepa* and *gp130StatΔhepa* mice showed impaired induction of acute-phase response genes and pronounced liver injury after concanavalin A–induced hepatitis (Klein et al., 2005). We found that hepatic gp130 deficiency severely decreased survival of *gp130Δhepa* mice during polymicrobial sepsis compared with control littermates (Fig. 1 A). Control mice carried loxP sites flanking exon 16 of the gp130 gene but did not express Cre recombinase (*gp130f/f*). The protective effects of hepatic gp130 signaling required STAT3 activation, demonstrated by a markedly decreased survival of *gp130StatΔhepa* compared with *gp130f/f* and *gp130RasΔhepa* animals (Fig. 1 B). STAT3 was strongly phosphorylated in the liver after CLP in *gp130f/f* and *gp130RasΔhepa* mice but not in *gp130Δhepa* and *gp130StatΔhepa* mice (Fig. 1 C), demonstrating a strict gp130 dependency of hepatic STAT3 phosphorylation during infection. Proinflammatory cytokines such as IL-6, TNF, and IFN-γ are heavily involved in the pathogenesis of septic shock and subsequent organ failure (Hotchkiss and Karl, 2003). In our mouse model, serum levels of these cytokines

peaked similarly at 6 h in all animals (unpublished data). In contrast, although the systemic cytokine levels quickly normalized in *gp130f/f* control and *gp130RasΔhepa* mice, they remained persistently elevated after 24 and 48 h in *gp130Δhepa* and *gp130StatΔhepa* animals (Fig. 1 D). Interestingly, it has been reported that patients with liver cirrhosis have strongly elevated sepsis-related mortality and show prolonged elevation

of IL-6 and TNF serum levels several days after the onset of sepsis (Byl et al., 1993).

Based on these findings, we explored the possibility of defective bacterial clearance in mice lacking hepatic gp130–STAT3 signaling leading to elevated cytokine levels, because we had previously observed that systemic inducible gp130 deficiency increased bacterial translocation during cholestasis
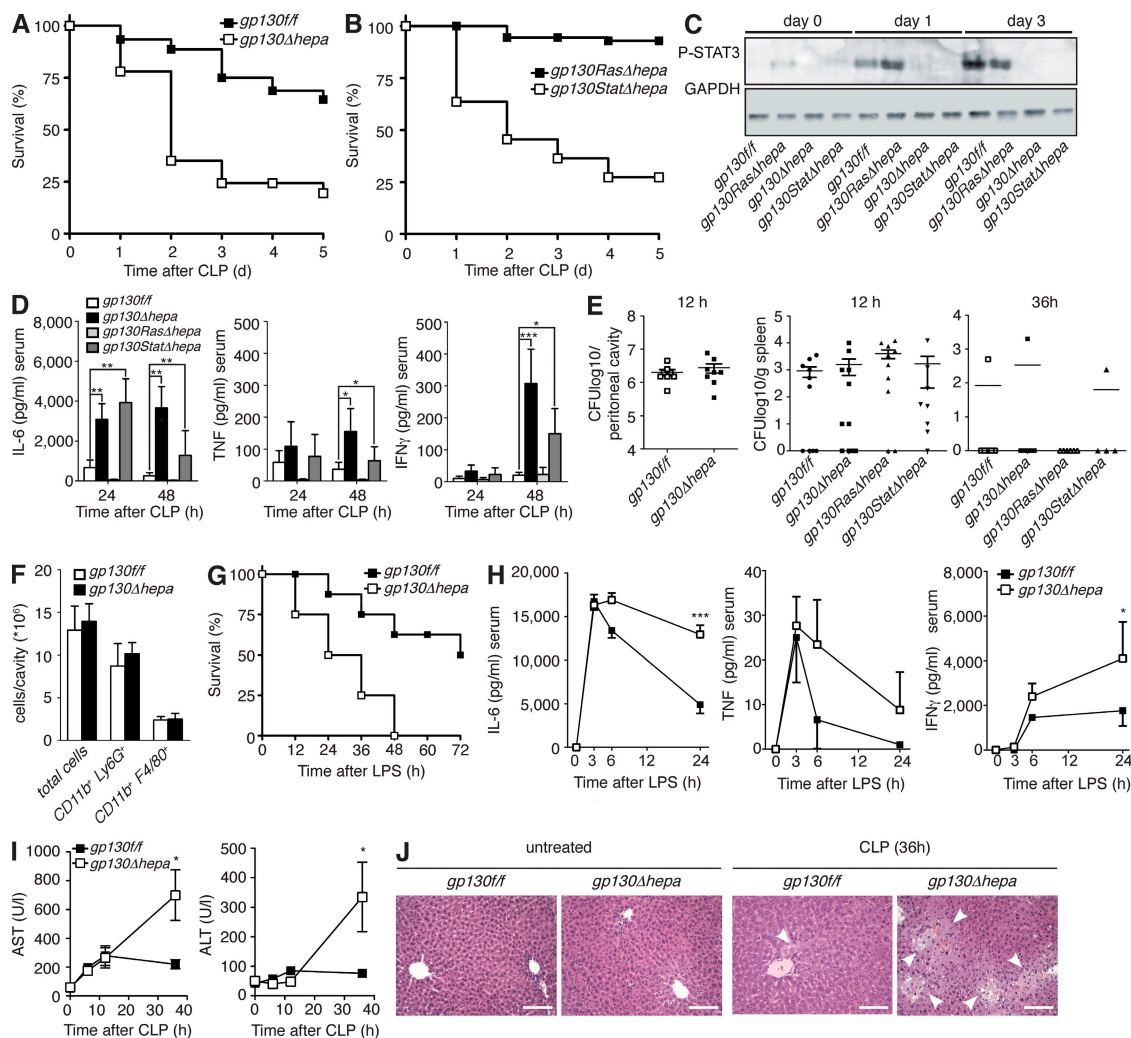

Figure 1.   gp130–STAT3 signaling in hepatocytes is protective during polymicrobial sepsis and tempers the inflammatory response.
(A) Decreased survival of *gp130Δhepa* mice after CLP (*n* = 45 per group; pooled data of six independent experiments). (B) Decreased survival of *gp130StatΔhepa* mice compared with *gp130RasΔhepa* mice after CLP (*n* = 18 per group; pooled data of three independent experiments). (C) Western blot for phospho-STAT3 (P-STAT3) in lysates of liver samples taken at the indicated time points. (D) Serum cytokine levels in *gp130Δhepa* and *gp130StatΔhepa* mice compared with controls. IL-6, TNF, and IFN-γ were measured by ELISA in serum samples collected at the indicated time points after CLP (*n* = 10 per group; pooled data of three independent experiments). (E) Bacterial burdens in the peritoneal cavity (left) and in spleens (right) were determined 12 and 36 h after CLP by plating serial dilutions of peritoneal lavage fluid or spleen tissue homogenate on agar plates. CFUs were counted after overnight incubation (*n* = 8–10 per group; pooled data of three independent experiments). (F) Recruitment of immune cells to the peritoneal cavity in *gp130Δhepa* and control mice. Peritoneal cavities were lavaged 18 h after CLP, and infiltrating cells were counted and analyzed by flow cytometry. CD11b+Ly6G+, neutrophils; CD11b+F4/80+, monocytes and macrophages (*n* = 5 per group; one out of three independent experiments is shown). (G) Endotoxic shock was induced by injection of 20 mg/kg LPS and survival was determined (*n* = 10 per group; pooled data of three independent experiments). (H) Serum cytokine concentrations in *gp130f/f* and *gp130Δhepa* mice after LPS treatment were measured by ELISA (*n* = 8 per group; pooled data of three independent experiments). (I) Serum concentrations of aspartate transaminase (AST; left) and alanine transaminase (ALT; right; *n* = 5 per group; one out of three independent experiments is shown). (J) Representative hematoxylin and eosin staining of histological sections of liver tissue. Bars, 100 μm. *, P < 0.05; **, P < 0.01; ***, P < 0.001. Data are presented as means ± SEM.

after bile-duct obstruction (Wuestefeld et al., 2003). However, when we examined bacterial counts of the peritoneal cavity and the spleen by plating serial dilutions of peritoneal lavage fluid or spleen homogenates 12 h after CLP, we found no differences between the groups and nearly all animals had cleared the bacteria from the spleens after 36 h (Fig. 1 E). Furthermore, leukocyte recruitment to the peritoneal cavity was equal in all groups (Fig. 1 F), indicating that the innate immune response was intact. This suggested that impaired counterregulation of the initial inflammatory response rather than defective antibacterial defense was responsible for the exacerbated inflammation and increased mortality of *gp130∆hepa* mice. To further validate this hypothesis, we induced sterile endotoxic shock by injection of LPS. Similar to the infection model, hepatic gp130 deficiency strongly increased mortality (Fig. 1 G) and caused prolonged inflammation (Fig. 1 H). We also evaluated the liver-intrinsic effects of gp130 deficiency during sepsis and found that *gp130∆hepa* mice showed markedly elevated liver enzyme serum levels (Fig. 1 I) and pronounced hepatocyte necrosis (Fig. 1 J) compared with *gp130f/f* mice after CLP. Enhanced liver injury not only reflected the severity of the systemic inflammation but also confirmed the autoprotective function of IL-6–gp130 signaling in hepatocytes. Collectively, these experiments suggested that liver-derived gp130-dependent factors were essential to control the inflammatory response to infection.

Hepatic gp130 signaling is required for mobilization and accumulation of MDSCs

We next asked whether dysregulated inflammation in *gp130∆hepa* mice was associated with changes in the composition of immune cells in the peripheral blood, lymphoid organs, and the liver. We especially focused on MDSCs, an immature population of myeloid (precursor) cells characterized by surface expression of CD11b and Gr1. MDSCs have recently gained significant attention for their role in malignancies. Interestingly, one previous study reported expansion of MDSCs in the bone marrow and accumulation in the spleens of septic mice (Delano et al., 2007). We therefore monitored the expansion of CD11b$^+$Gr1$^+$ cells in the bone marrow, as well as their mobilization to the peripheral blood and accumulation in the spleens, lymph nodes, and livers of mice at various time points after induction of polymicrobial sepsis. We found that although CD11b$^+$Gr1$^+$ cells expanded similarly in the bone marrow of all mice, the population of circulating CD11b$^+$Gr1$^+$ cells in the blood was significantly reduced in *gp130∆hepa* mice (Fig. 2, A and B). We observed the accumulation of MDSCs in the spleens of septic *gp130f/f* control mice, as previously reported (Fig. 2, A–C; Delano et al., 2007). However, splenic enrichment of MDSCs after CLP was completely blocked in *gp130∆hepa* animals, as demonstrated by flow cytometry and immunofluorescence microscopy (Fig. 2, A–C). Hepatic accumulation of CD11b$^+$Gr1$^+$ cells was also significantly decreased in *gp130∆hepa* mice (Fig. S1 A). In agreement with a previous study (Delano et al., 2007), no increase of MDSCs in mesenteric lymph nodes was observed

in any of the animals (Fig. S1 B). These data strongly suggested that gp130-dependent signals in the liver facilitated mobilization and peripheral accumulation of MDSCs during polymicrobial sepsis.

CD11b$^+$Gr1$^+$ MDSCs regulate innate inflammation and confer protection during sepsis

Positive CD11b/Gr1 staining is not unique to MDSCs, especially in compartments with relatively high numbers of myeloid cells such as the bone marrow and the peripheral blood. The population of CD11b$^+$Gr1$^+$ cells is therefore not equivalent to MDSCs, but it also includes neutrophils and monocytes at various stages of maturation. In the absence of exclusive surface markers, MDSCs are best defined functionally, through their ability to suppress immune responses. Therefore, we analyzed their functions during sepsis and sought to investigate a possible link between hepatic gp130 deficiency, subsequent impairment of MDSC accumulation, and reduced survival. We chose two independent approaches to test the relevance of MDSCs for host survival. First, we depleted Gr1$^+$ MDSCs in control mice using a monoclonal antibody directed against Gr1. Depletion of MDSCs significantly increased mortality compared with mice treated with a control isotype antibody (Fig. 3, A and B). Because anti-Gr1 treatment is not specific for MDSCs and would also target other Gr1$^+$ cells like neutrophils, we decided to adoptively transfer MDSCs, isolated from spleens of *gp130f/f* donors 5 d after CLP, into *gp130∆hepa* animals. Purified MDSCs from spleens of *gp130f/f* mice showed a characteristic morphological heterogeneity and immature phenotype (Fig. 3, C and D). Approximately 50% of CD11b$^+$Gr1$^+$ cells expressed Ly6G, a neutrophil marker that has been associated with the PMN subset of MDSCs (Fig. 3 C). Importantly, MDSCs efficiently reversed the detrimental effects of hepatic gp130 deficiency during infection (Fig. 3 E). MDSC transfer increased survival of *gp130∆hepa* mice to wild-type levels (Fig. 3 E) and normalized the serum levels of proinflammatory cytokines in *gp130∆hepa* mice (Fig. 3 F), thus demonstrating a key role of MDSCs in regulating inflammatory responses to infection. Previous studies had shown suppressive effects of MDSCs on T cells (Delano et al., 2007; Movahedi et al., 2008). We found that purified sepsis-induced splenic MDSCs inhibited LPS-induced proinflammatory cytokine release while strongly inducing the production of IL-10 in primary macrophages (Fig. 3, G–I). This skewing effect was dependent on activation of the MDSCs in vivo. CD11b$^+$Gr1$^+$ cells that were sorted from the spleens of untreated mice were impaired in their ability to inhibit IL-12 release and to induce IL-10 production in LPS-treated macrophages (Fig. 3 H). Preactivation of CD11b$^+$Gr1$^+$ cells from naive mice with LPS in vitro before co-culture with macrophages partially restored IL-10 induction but failed to recover inhibition of IL-12 production (Fig. 3 H). Thus, MDSCs generated during infection show a strong antiinflammatory phenotype, in contrast to splenic CD11b$^+$Gr1$^+$ cells under steady-state conditions. The antiinflammatory functions of MDSCs were largely dependent
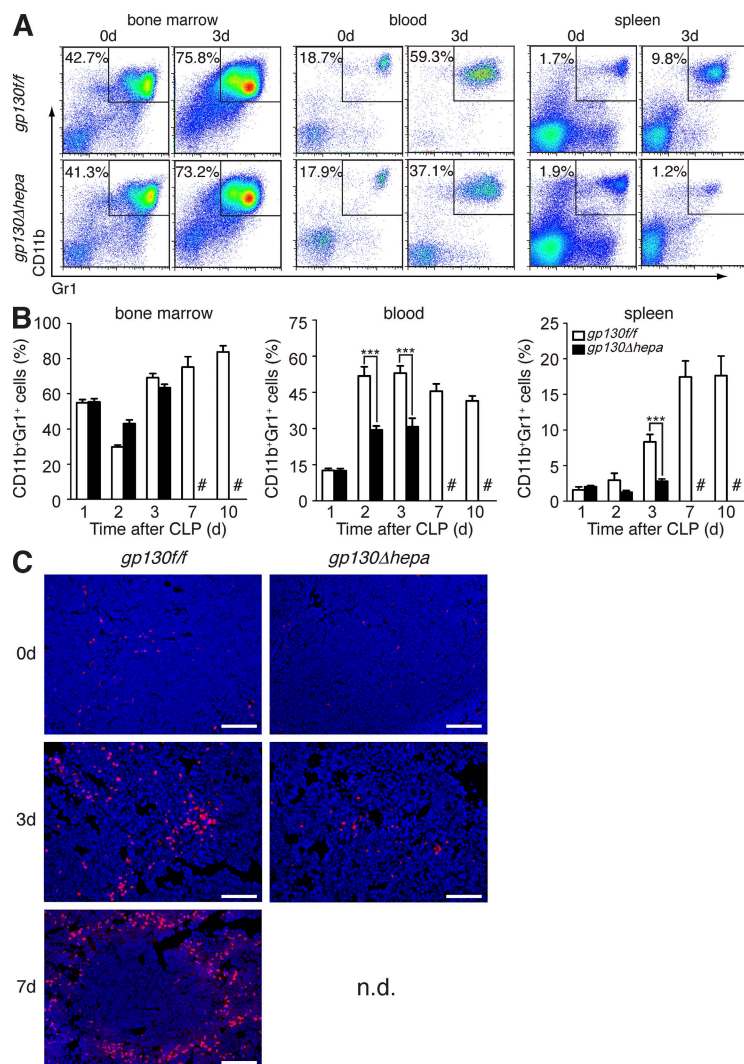
Figure 2. Mobilization and splenic accumulation of CD11b+Gr1+ MDSCs are impaired in *gp130Δhepa* mice. (A) Representative flow cytometric analysis and (B) graphic analysis of CD11b+Gr1+ cell frequencies in bone marrow, peripheral blood, and spleens in *gp130f/f* and *gp130Δhepa* mice at the indicated time points after CLP (*n* = 5–12 per time point per group; pooled data of 12 independent experiments). #, *gp130f/f* did not survive to 7 and 10 d in sufficient numbers and could therefore not be included in the analysis. (C) Immunofluorescence staining of spleen sections for CD11b (red, CD11b; blue, DAPI) to show infiltration of myeloid cells after induction of sepsis. Spleens were explanted at the indicated time points. Bars, 100 µm. ***, P < 0.001. Data are presented as means ± SEM. n.d., not determined.

proteins, we noticed three groups of genes with a particularly strong gp130-dependent induction: (1) classical APPs such as α2-macroglobulin or SAA; (2) chemokines with chemotactic activity on myeloid cells, such as Cxcl1 (KC), Cxcl2, or Ccl3 (MIP-1α); and (3) antiinflammatory cytokines such as IL-1R antagonist (IL-1Ra; Fig. 4 A and Fig. S2). These results were further confirmed by real-time RT-PCR (Fig. 4 B). Accordingly, the serum levels of SAA and KC were strongly elevated in *gp130f/f* but not in *gp130Δhepa* mice 24 h after CLP, showing that hepatic gp130 signaling controls the systemic levels of these proteins (Fig. 4 C). Transcript levels of IL-6 were also significantly reduced in *gp130Δhepa* mice compared with controls (8.3- vs. 1.9-fold induction; unpublished data), which is noteworthy because it is widely believed that the liver is a major source of IL-6 and TNF during sepsis (Matuschak, 1996). In contrast, we found that *gp130Δhepa* mice showed elevated serum levels of IL-6 after CLP despite reduced hepatic IL-6 production (Fig. 1 D). Hepatic TNF transcription was not differentially regulated by gp130 (unpublished data). This suggests a mainly extrahepatic production during sepsis, e.g., in macrophages activated by microbial products.

Having identified hepatic genes regulated by gp130 during polymicrobial infection, we aimed to determine their functional contributions to the regulation of the inflammatory response and MDSC accumulation. To this end, we treated *gp130Δhepa* mice that failed to induce SAA, KC, and IL-1Ra with the respective recombinant proteins. Administration of SAA or KC alone partly restored survival (Fig. 5, A and B), whereas a combination of both proteins completely rescued *gp130Δhepa* mice, normalizing survival rates and systemic cytokine levels (Fig. 5, A, B, D, and E). In sharp contrast, treatment with the antiinflammatory cytokine IL-1Ra (anakinra) resulted in 100% mortality of *gp130Δhepa* mice after 4 d (Fig. 5 C). Detrimental effects of IL-1Ra treatment may be caused by impaired bacterial clearance or defective tissue repair in the absence of IL-1R signaling.

on direct cell–cell contact. Separation of MDSCs and macrophages in a Transwell system strongly reduced IL-10 induction but only partially blocked IL-12 suppression (Fig. 3 I), indicating that additional soluble factors such as TGF-β may play a role as well. Our results suggest that direct interaction of MDSCs with innate effector cells may constitute a novel autoregulatory mechanism of innate immune responses to infection.

Liver–derived serum amyloid A (SAA) and KC control inflammation and promote MDSC mobilization and accumulation

Next we aimed to identify liver-derived gp130-dependent factors that were involved in mobilization and peripheral accumulation of MDSCs, thereby controlling inflammation. Transcriptional analysis of 16,475 genes by gene microarray in liver tissue samples taken from untreated and septic *gp130f/f* and *gp130Δhepa* mice revealed a total of 3,936 genes that were regulated >1.5-fold 12 h after CLP, 2,266 of which were differentially regulated by gp130. Focusing on secreted

Notably, administration of recombinant KC, known as a potent chemoattractant for polymorphonuclear cells (Bozic et al., 1995), significantly elevated the number of circulating CD11b^{+}Gr1^{+} cells in septic gp130Δhepa mice (Fig. 6 A). Recombinant KC also induced chemotaxis of purified MDSCs in vitro (Fig. S3). In contrast, splenic MDSC numbers were only marginally elevated in KC-treated gp130Δhepa animals (Fig. 6 B). Thus, it was conceivable that KC was involved in mobilization of myeloid cells from the bone marrow, whereas accumulation of MDSCs in the spleen required additional factors. We therefore tested the ability of SAA to restore splenic MDSCs. SAA is mostly regarded as a proinflammatory protein with activating properties on innate immune cells (Badolato et al.,

1994; Cheng et al., 2008a), and has also been implicated in the pathogenesis of chronic inflammation such as atherosclerosis (Luchtefeld et al., 2007). SAA treatment of gp130Δhepa mice during sepsis efficiently reduced mortality (Fig. 5, B and D) and inflammation (Fig. 5 E), but importantly, it nearly restored MDSC numbers in the spleen, especially when given in combination with KC (Fig. 6 B), demonstrating that SAA was sufficient to rescue gp130Δhepa mice during sepsis. However, it was not clear if SAA was required in the context of an intact acute-phase response. Blocking SAA activity in gp130f/f mice by injection of neutralizing anti-SAA antibodies strongly enhanced sepsis–related mortality and systemic cytokine levels (Fig. 5, F and G). Given the large quantities and vast variety
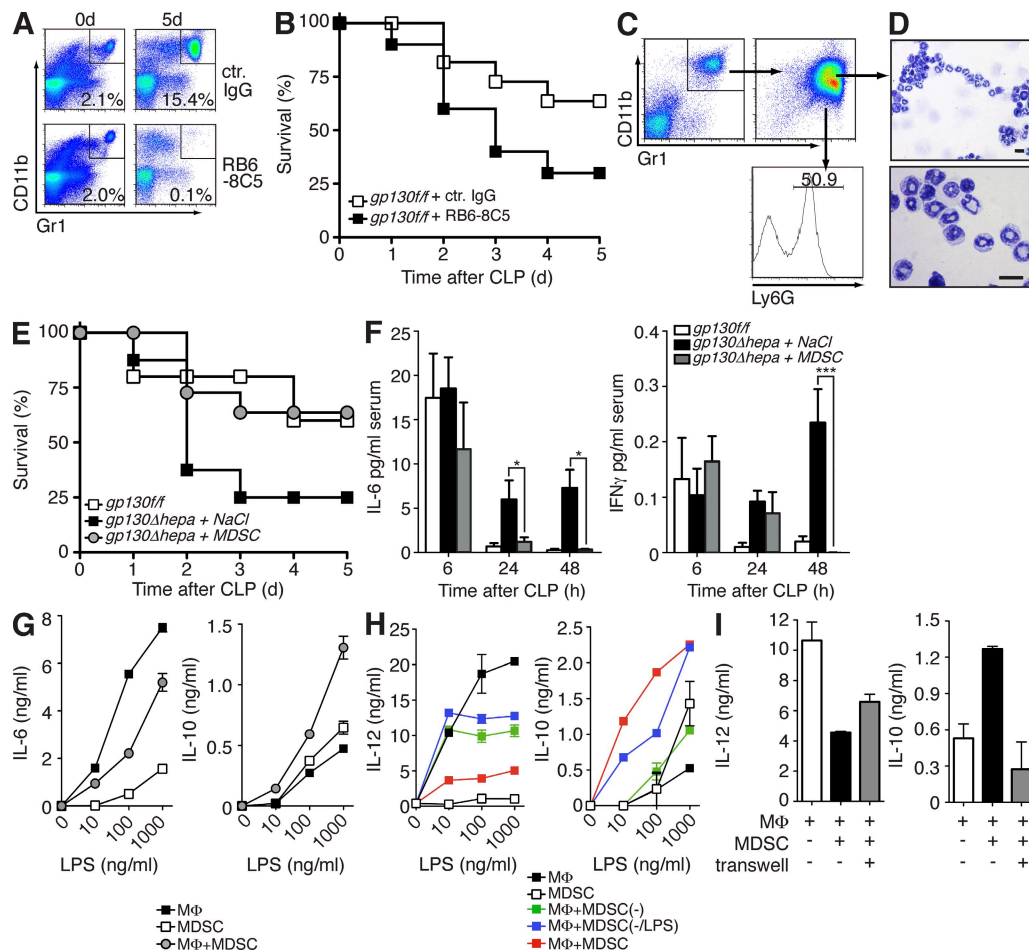

Figure 3. MDSCs regulate inflammatory responses and confer protection during sepsis. (A and B) gp130f/f mice were injected with monoclonal antibodies against Gr1 (RB6-8C5) 24 h before and after CLP. Efficient depletion of Gr1^{+} MDSCs was determined by flow cytometry of total splenocytes (A). Survival was monitored (B; n = 9 per group; pooled data of three independent experiments). (C) gp130f/f donor mice underwent CLP and 5 d later MDSCs were isolated from the spleens. CD11b^{+}Gr1^{+} purity of >90% was confirmed by flow cytometry (top right). Further analysis of Ly6G expression of MDSCs (bottom right). (D) Cytospins of MDSCs. Bars, 10 µm. (E) gp130Δhepa mice received either 5 × 10^{6} MDSCs or saline 1 and 24 h after CLP and survival was determined (n = 12 per group; pooled data of three independent experiments). (F) Serum samples were taken at the indicated time points and analyzed for IL-6 and IFN-γ by ELISA. (G) Peritoneal macrophages (MΦ) were co-cultured with MDSCs isolated from septic gp130f/f mice at a ratio of 1:3 and were stimulated with LPS at the indicated concentrations. Cytokine release was determined by ELISA (one out of five independent experiments shown). (H) Gr1^{+}CD11b^{+} cells were isolated from the spleens of septic mice (MDSC) or naive mice (MDSC(−)) and co-cultured with macrophages and stimulated with LPS. Some cells from naive mice were pretreated with 100 ng/ml LPS in vitro before co-culture with macrophages (MDSC(−/LPS)). (I) MDSCs and macrophages were separated in a Transwell and stimulated with LPS. Cytokine release was determined by ELISA (H and I; one out of three independent experiments shown). *, P < 0.05; ***, P < 0.001. Data are presented as means ± SEM.

of APPs produced during sepsis, we were surprised to find that inhibition of SAA alone had such dramatic effects, and it indicates a central role for this APP in the regulation of the inflammatory response to infection. Thus, hepatic APPs promote MDSC accumulation and regulate inflammation during sepsis.

Contraction of immune cells, particularly lymphocytes, by apoptosis during severe infections is a well-known phenomenon (Hotchkiss and Nicholson, 2006). We found a higher percentage of annexin V$^+$ apoptotic MDSCs in spleens of *gp130Δhepa* mice compared with *gp130f/f* mice (Fig. 6 C). Interestingly, the apoptotic fraction was significantly reduced in SAA-treated *gp130Δhepa* animals (Fig. 6 A). Thus, we reasoned that SAA promotes survival of peripheral MDSCs especially in light of a recent report suggesting an antiapoptotic function of SAA in neutrophils (Christenson et al., 2008). We therefore tested the potential of SAA to inhibit apoptosis of MDSCs isolated from spleens of septic mice. Indeed, we found that both recombinant SAA and supernatant of stimulated primary hepatocytes isolated from *gp130f/f* but not from *gp130Δhepa* mice prevented TNF-induced MDSC apoptosis (Fig. 6 D). Primary hepatocytes isolated from control *gp130f/f* and *gp130Δhepa* mice were stimulated with leukemia inhibitory factor, a strong gp130 agonist, to induce production of gp130-dependent proteins. Addition of SAA to the supernatant of

gp130Δhepa hepatocytes fully restored the antiapoptotic capacity (Fig. 6 D), demonstrating that liver-derived SAA, produced in response to gp130 activation, protects MDSCs from apoptosis. Therefore, SAA inhibits MDSC apoptosis in vitro and in vivo. Collectively, these results define a pivotal role of liver-derived proteins in regulating MDSC mobilization and survival in sepsis, and the production of these factors requires gp130–STAT3 signaling in hepatocytes.

DISCUSSION

Although the use of antibiotics dramatically decreased the mortality of bacterial infections in the last century, sepsis-related mortality has remained high, even with appropriate antibiotic therapy, fluid replacement, and organ function support (Angus et al., 2001; Hotchkiss and Karl, 2003). Thus, there is an urgent need for targeted sepsis therapies. Various approaches to inhibit major inflammatory mediators such as TNF, IL-1, leukotrienes, or the endotoxin component lipid A have been tested in clinical trials with largely discouraging results (Fisher et al., 1996; Parrish et al., 2008). In contrast, exploiting endogenous regulatory mechanisms may represent a more promising strategy (Parrish et al., 2008). In fact, the only sepsis treatment approved by the Food and Drug Administration in the United States is administration of activated protein C (Bernard et al., 2001), a plasma protein with
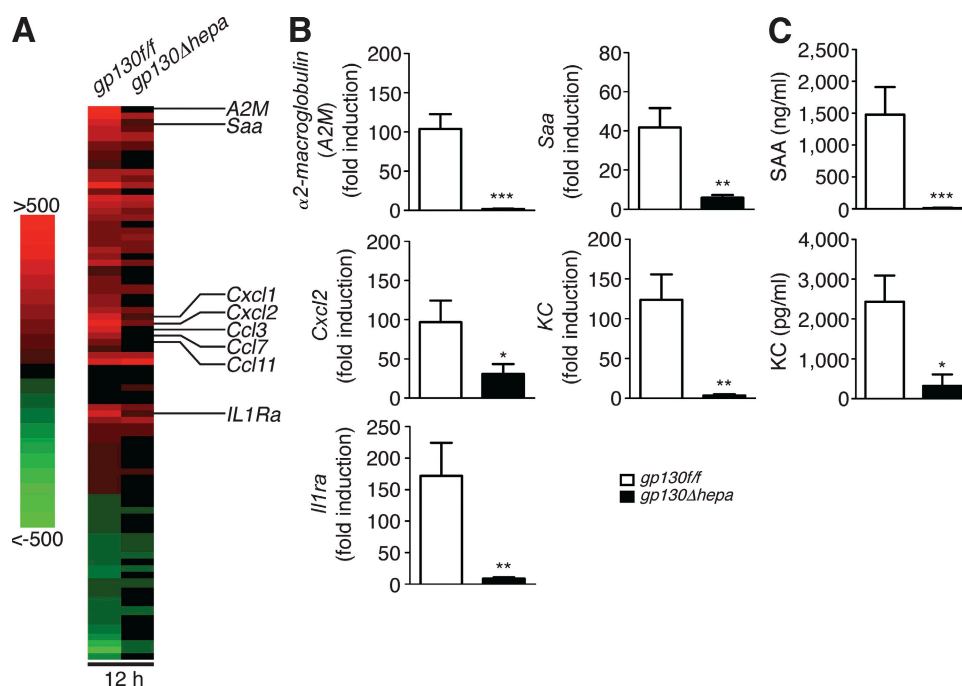
Figure 4. Hepatocytes launch a specific gp130–dependent transcriptional program in response to infection. (A) Gene microarray analysis of liver tissue before and 12 h after onset of polymicrobial sepsis (*n* = 3 per group). Genes with >1.5-fold change after CLP in three out of three samples were clustered in a heat map diagram. Red indicates up-regulation compared with control mice, and green indicates down-regulation; all genes with an absolute fold change <1.5 and/or a p-value >0.05 are shown as black (no change). (B) Quantitative real-time PCR of liver samples taken from untreated *gp130f/f* and *gp130Δhepa* mice and 12 h after induction of sepsis (*n* = 8 per group; pooled data of three independent experiments). APPs (α2-macroglobulin and SAA), chemokines (KC and Cxcl2), and antiinflammatory cytokines (IL-1Ra) were analyzed. (C) Serum protein levels of SAA (top) and KC (bottom) were analyzed by ELISA in *gp130f/f* and *gp130Δhepa* mice 24 h after CLP (*n* = 7 per group; three independent experiments). *, P < 0.05; **, P < 0.01; ***, P < 0.001. Data are presented as means ± SEM.

anticoagulant and antiinflammatory functions. Its proform protein C is produced in the liver. In the current study, we found that hepatic APPs, namely SAA and KC, were protective during sepsis and promoted the function of MDSCs. MDSCs were capable of controlling inflammatory responses and reducing mortality in a mouse model of polymicrobial sepsis. Myeloid cells with antiinflammatory functions have been recognized in tumor-bearing mice for a long time (Young et al., 1987), but their functional significance for tumor immune evasion, angiogenesis, and metastasis has only recently gained broader attention (Nagaraj et al., 2007; Yang et al., 2008). MDSCs have also been implicated in other pathological conditions such as autoimmunity (Zhu et al., 2007; Haile et al., 2008). However, despite significant advances in cancer, there is only limited data on MDSC functions in infections and sepsis. Expansion of MDSCs with T cell–suppressive properties during sepsis in mice has been reported (Delano et al., 2007), but unlike for many cancers, their contribution to disease progression and host survival during infections remained undefined. In this paper, we demonstrate that MDSCs display host-protective antiinflammatory functions during polymicrobial infection. *gp130Δhepa* animals that failed to accumulate MDSCs in the spleen suffered from dysregulated inflammation and increased mortality, whereas adoptive transfer of splenic MDSCs into *gp130Δhepa* mice conferred protection. It is known that adaptive immune cells are required to control innate immune responses to infections (Kim et al., 2007). As shown in this study and previously with cancer-derived MDSCs (Sinha et al., 2007), MDSCs can directly interact with macrophages and

inhibit proinflammatory cytokine release. Thus, they represent an autoregulatory component of the innate immune system, contributing to carefully balance the inflammatory response to bacterial infection and sepsis.

Knowledge about factors and conditions that induce MDSC production and function as well as their homing to peripheral tissues or lymphoid organs is incomplete. Observations made in mouse cancer models have suggested that tumor-derived factors induce the expansion of MDSCs and inhibit their differentiation into dendritic cells by activation of JAK2–STAT3 pathways in MDSCs (Nefedova et al., 2004). In our model, JAK2–STAT3 signaling in hematopoietic cells was intact and we thus observed no differences in MDSC expansion in the bone marrow. Instead, hepatocyte-specific deletion of gp130–STAT3 signaling abrogated the peripheral accumulation of MDSCs. We found that gp130-dependent production of SAA and KC in the liver cooperatively facilitated MDSC mobilization and survival. However, how MDSCs home to the spleen and not to other lymphoid organs like the mesenteric lymph node is not clear at this point. A previous study reported that STAT3-inducible myeloid-related protein S100A9 induced MDSC production in cancer, leading to inhibition of antitumor responses (Cheng et al., 2008b). Interestingly, we found a 39-fold increase in S100A9 gene expression in livers of *gp130f/f* mice versus an 8-fold induction in *gp130Δhepa* mice (unpublished data), suggesting that the liver might be a potent source of MDSC-inducing proteins not only during infections but potentially also in cancer. In this respect, it is also noteworthy that MDSCs have been shown to accumulate in human hepatocellular
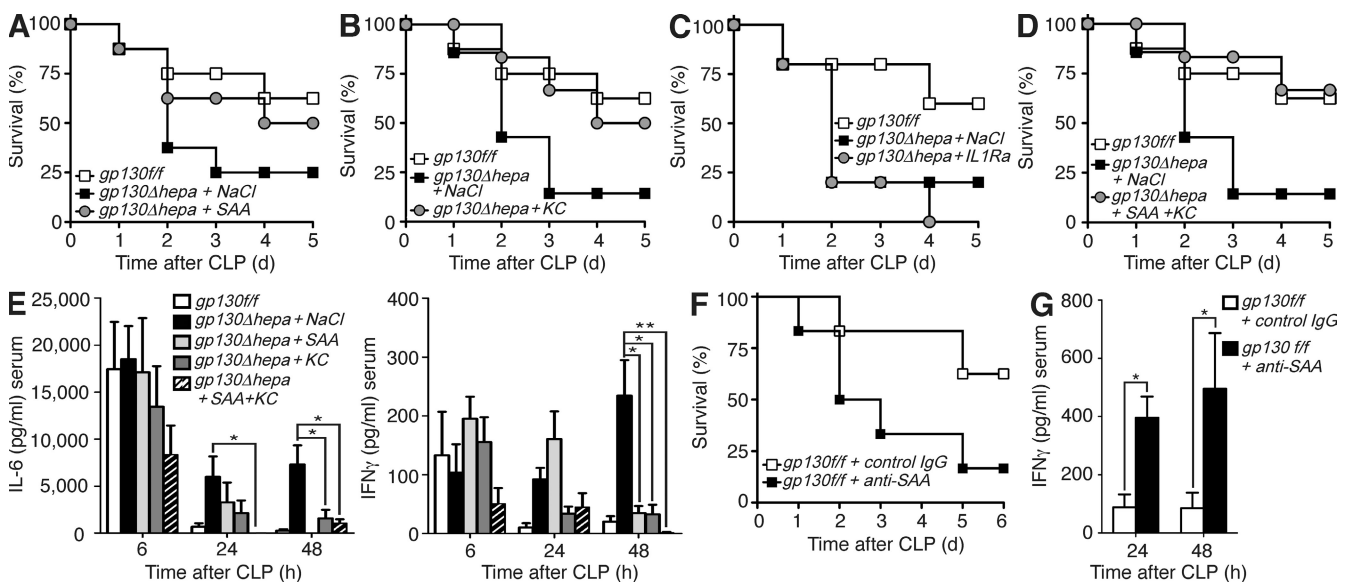
Figure 5.   Recombinant SAA and KC are protective during sepsis. (A–D) Survival of *gp130f/f* mice compared with *gp130Δhepa* mice treated with SAA (A), KC (B), IL-1Ra (anakinra; C) or SAA and KC (D) in combination or equal volumes of NaCl 1 and 24 h after CLP (*n* = 9 per group; pooled data of three independent experiments). (E) Serum concentrations of IL-6 (left) and IFN-γ (right) at the indicated time points measured by ELISA. (F) Survival of *gp130f/f* mice treated with neutralizing anti-SAA antibodies or inactive control isotype IgG. (G) IFN-γ serum concentrations at the indicated time points after CLP in *gp130f/f* mice treated with anti-SAA or control antibodies (*n* = 6 per group; pooled data of two independent experiments). *, P < 0.05. Data are presented as means ± SEM.

carcinoma, a cancer known to notoriously escape antitumor immune responses (Hoechst et al., 2008). Moreover, a recent study demonstrates frequent gain-of-function mutations in the gp130 gene in liver tumors (Rebouissou et al., 2009). Future investigations should therefore determine the role of gp130–STAT3 activation in the liver for MDSC regulation in different pathological conditions including cancer. Because MDSCs represent a heterogeneous population, it is conceivable that phenotype and function as well as activating factors differ between the various conditions in which they are found. Although the role of JAK2–STAT3 for MDSC induction has been studied mainly in malignancies, it was previously shown that the expansion of MDSCs during polymicrobial sepsis required MyD88 signaling (Delano et al., 2007). However, it is not clear if direct MyD88 activation in MDSCs or, alternatively, indirect mechanisms like

MyD88-dependent production of cytokines such as IL-6 are responsible for these effects. Our present study does not directly address this issue, but the results demonstrate that MyD88–NF-κB–dependent IL-6 cytokines and subsequent gp130 signaling in hepatocytes are crucial elements for peripheral accumulation of MDSCs during sepsis. This concept is intriguing because it would implicate a novel negative feedback mechanism of Toll-like receptor (TLR)–mediated inflammatory responses. We found that among all APPs, SAA played a pivotal role in regulating inflammatory responses and survival. Interestingly, SAA was recently identified as an endogenous TLR2 ligand activating MyD88 signaling (Cheng et al., 2008a). It is therefore conceivable that SAA activates TLR2–MyD88 in MDSCs to protect them from apoptosis. This explanation would also support the previously reported requirement for MyD88 for MDSC expansion during sepsis (Delano et al., 2007).

Our present study demonstrates that MDSCs have potent host-protective antiinflammatory functions during polymicrobial infection, and our results directly link MDSC functions during infection to hepatic APPs induced by gp130–STAT3 activation. We show that APPs are crucial regulators of inflammatory responses to infection, highlighting the close relationship between hepatocytes and innate immune cells, and SAA plays a key role in this regulatory process. In conclusion, the present study adds important information to our current understanding of the role of the liver and hepatic APPs in regulating inflammatory responses and maintaining immune homeostasis during infection.

MATERIALS AND METHODS

Mice. We used 8–12-wk-old male *gp130f/f*, *gp130Δhepa*, *gp130StatΔhepa*, and *gp130RasΔhepa* mice, as described previously (gp130 mutant mice were provided by M. Ernst, Ludwig Institute for Cancer Research, Victoria, Australia; Klein et al., 2005). All experiments were approved by the Institutional Animal Care and Use Committee of the RWTH University Hospital. All experiments were performed in agreement with the Guide for the Care and Use of Laboratory Animals (National Institutes of Health publication no. 86-23, revised 1985).

CLP. We induced polymicrobial sepsis by CLP (Rittirsch et al., 2009). In brief, mice were anesthetized, and the cecum was ligated and punctured twice with a 20-gauge needle. We monitored mice every 6 h for 24 h and then every 12 h until the end of the experiment (between 5 and 10 d).

LPS-induced endotoxic shock. Mice received 20 mg/kg LPS i.p. and were monitored every 6 h for 24 h and then every 12 h until the end of the experiment (between 3 and 5 d).

Cell isolation and culture. We isolated MDSCs from spleens of *gp130f/f* mice 5 d after CLP. After sacrifice, spleens were explanted and splenocytes were isolated by collagenase digestion. Red blood cells were lysed using lysing buffer (Pharmlyse; BD). MDSCs were purified from cell suspensions by magnetic cell sorting (MACS; Miltenyi Biotec) using anti-CD11b–conjugated magnetic beads (Miltenyi Biotec). Purity was determined by flow cytometry. We used only cell preparations with a purity >90% for further experiments. Alternatively, mice were injected with 5 mg/kg LPS i.p., and 5 d later CD11b+Gr1+ splenocytes were purified by FACS sorting (Influx; BD). For overnight culture experiments, cells were kept in RPMI 1640 (Invitrogen) supplemented with 10% heat-inactivated FCS (Sigma-Aldrich). MDSCs were
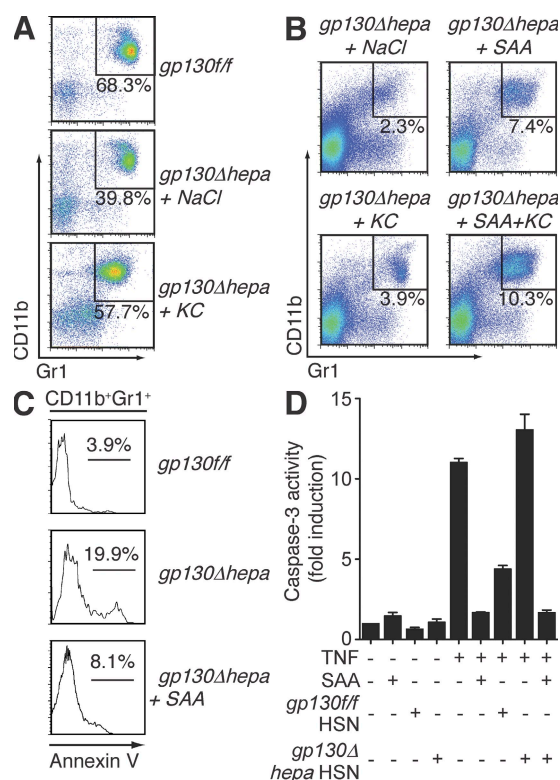

Figure 6. Hepatocyte–derived SAA reconstitutes splenic MDSCs and protects them from apoptosis. (A) Representative flow cytometric analysis of white blood cells from *gp130f/f* and *gp130Δ hepa* mice treated with NaCl or KC 5 d after CLP. (B) MDSCs measured in spleens from *gp130Δ hepa* mice treated with the indicated compounds 5 d after CLP. The percentage of CD11b+Gr1+ cells is indicated. (C) Annexin V staining of CD11b+Gr1+ cells indicating the fraction of apoptotic MDSCs in the spleen. (D) In vitro apoptosis of MDSCs induced by TNF can be inhibited by SAA or supernatants from primary hepatocytes isolated from *gp130f/f* (*gp130f/f* HSN) but not from *gp130Δ hepa* (*gp130Δ hepa* HSN) mice. Hepatocytes were stimulated with the potent gp130 ligand leukemia inhibitory factor for 6 h. Apoptosis of MDSCs was determined by measuring caspase-3 activity (one out of three independent experiments is shown). Data are presented as means ± SEM.

cultured with the following substances: mouse TNF (PeproTech), LPS (Sigma-Aldrich), and SAA (PeproTech).

For generation of peritoneal macrophages, we injected mice with 1 ml thioglycollate (BD) i.p. Total cells were harvested after 72 h and plated at 10^6 cells/ml in RPMI 1640 supplemented with 10% FCS and 1% penicillin/streptomycin (Invitrogen). After overnight culture, nonadherent cells were removed and purity of macrophages was confirmed by F4/80 staining and flow cytometry.

Primary hepatocytes were isolated from *gp130f/f* and *gp130Δhepa* mice by collagenase perfusion as described previously (Klein et al., 2005). 10^6 cells were cultured on 6-cm culture plates with DMEM (Invitrogen) containing 4.5 g/liter glucose, 10% FCS, and penicillin/streptomycin overnight. Cells were stimulated with 50 ng/ml leukemia inhibitory factor (PeproTech) for 6 h, and supernatants were harvested and stored at −80°C.

In vitro culture of MDSCs. Culture conditions have been used previously (Delano et al., 2007). After MACS purification of splenic MDSCs from control *gp130f/f* mice 5 d after CLP, cells were plated at 10^6 cells/ml in RPMI 1640 supplemented with 10% FCS, 2 mM L-glutamine, 200 U/ml penicillin, and 50 µg/ml streptomycin and cultured overnight with the compounds indicated in the figures. For in vitro suppression assays, purified MDSCs were co-cultured with peritoneal or bone marrow–derived macrophages and stimulated with LPS, and subsequent cytokine release was measured by ELISA. In some cases, MDSCs were separated from macrophages in Transwells (pore size = 0.4 µm; Corning) For in vitro migration studies, splenic or bone marrow–derived CD11b⁺Gr1⁺ cells were seeded in Transwells (pore size = 3 µm; Corning), and increasing amounts of recombinant KC (PeproTech) were added to the lower well. After 3 h, migrated cells were counted in a hemocytometer and the migration index of migrated/nonmigrated cells was calculated.

Adoptive MDSC transfer. MDSCs were isolated as described in Cell isolation and culture, and *gp130Δhepa* mice received 5 × 10^6 MDSCs i.v. 1 and 24 h after CLP. Control mice were treated with equal volumes of NaCl.

Depletion of Gr1⁺ cells. We generated monoclonal antibodies against Gr1 from RB6-8C5 hybridoma cells, and *gp130f/f* mice received 10 mg/kg of antibodies 24 h before and 24 h after CLP. Efficiency of depletion was monitored by FACS. Control mice received nonspecific isotype IgG antibodies.

Treatment of animals with recombinant SAA, KC, and IL-1Ra. Mice received 0.8 mg/kg recombinant SAA or 40 µg/kg KC or a combination of both i.v. 1 and 24 h after CLP. Control mice received the same volume of saline. IL-1Ra (anakinra; Kineret; Amgen) was injected subcutaneously every 4 h over a period of 24 h.

Systemic neutralization of SAA. Mice received 50 mg/kg of a combination of anti-SAA monoclonal antibodies (mc29 and mc4; 1:1) directed against the highly conserved (invariant) region of SAA i.p. 12 h before and 33 mg/kg 12 h after CLP. Control mice received equivalent amounts of inactive control antibodies (mc1).

Cytokine measurements. Serum samples were collected by bleeding at the time points indicated in the figures. IL-6, TNF, IFN-γ, and KC were measured by ELISA (R&D Systems). SAA was measured by ELISA (Invitrogen). IL-6, TNF, IL-12, and IL-10 were measured from cell-culture supernatants by ELISA (R&D Systems).

Flow cytometry. Cell suspensions were incubated with the following fluorochrome-conjugated antibodies and analyzed with a FACSCanto II (BD): CD45, Gr1 (both from BD), and CD11b (eBioscience).

Gene microarray analysis and real-time PCR. *gp130f/f* and *gp130Δhepa* mice were sacrificed without previous treatment or 12 h after CLP. Livers were explanted and tissue samples were frozen immediately. Liver RNA

samples from three mice per experimental group were used for microarray analysis. RNA samples were prepared and hybridized on GeneChip Mouse Genome 430 2.0 arrays (Affymetrix). Gene expression levels were calculated applying the GeneChip content-corrected robust multichip average algorithm and a remapped GeneChip description file. Differentially expressed genes were identified using Limma statistics. Genes with a corrected p-value similar or <0.05 and/or fold change >1.5 or less than −1.5 were considered significantly regulated. Ingenuity Pathway Analysis (version 5.5; Ingenuity Systems) and ErmineJ Gene Score Resampling were used to identify the most significantly changed canonical signaling pathways or gene ontology biological processes in *gp130f/f* and *gp130Δhepa* mice 12 h after sepsis onset, using a p-value similar to or <0.05 as input criteria. Fold changes of selected genes were visualized in a heat map diagram. Microarray data have been deposited in the Gene Expression Omnibus under accession no. GSE22009.

Real-time PCR analysis was performed to confirm data from the gene array. RNA was isolated using RNeasy columns (QIAGEN) according to the manufacturer's instructions. First-strand synthesis was performed with Oligo dT primers and reverse transcription was performed with reverse transcriptase (M-MLV; Invitrogen). Quantitative real-time PCR was performed using SYBR Green reagent (Invitrogen) in a real-time PCR system (Prism 7300; Applied Bioscience). Reactions were performed in duplicate and GAPDH values were used to normalize gene expression.

Histology. Mice were sacrificed at the time points indicated in the figures. 5-µm cryosections of spleens were stained with rat anti–mouse CD11b monoclonal antibody and DAPI (both from BD).

Western blot analysis. Protein extracts were separated on a 10% SDS–polyacrylamide gel and transferred to nitrocellulose membranes (Whatman). Membranes were blocked with 5% milk in PBS and probed with phospho-STAT3 (Cell Signaling Technology) and GAPDH (Biogenesis) antibodies.

Determination of bacterial burden. Mice were sacrificed 24 h after CLP. The peritoneal cavity was lavaged and the lavage fluid was plated on blood and MacConkey agar plates in serial dilutions. Spleens were removed, homogenized, and plated in serial dilutions on agar plates. CFUs were counted after overnight incubation.

Determination of apoptosis by caspase-3 kinase activity. Purified MDSCs were cultured overnight with the indicated compounds. Cells were washed and lysed at 4°C in 5 mmol/liter Tris/HCl, pH 8, 20 µmol ethylenediaminetetraacetic acid, 0.5% Triton X-100. Lysates were clarified by centrifugation at 13,000 *g* for 10 min. The reaction mixture contained 30 µg of cellular lysates, 1,000 µl of assay buffer (20 mmol/liter Hepes, pH 7.5, 10% glycerol, 2 mM dithiothreitol), and 20 mM caspase-3 substrate (Ac-DEVD-AMC; BD). After 2 h of incubation in the dark, enzymatic activity was measured in a luminescence spectrophotometer (LS-50; PerkinElmer).

Determination of apoptosis by annexin V staining. Cells were stained for CD45, Gr1, and CD11b, followed by incubation with annexin V–FITC (BD), and were analyzed by flow cytometry.

Statistical analysis. Statistical significance was determined by an unpaired two-tailed Student's *t* test implemented in Excel (version 11.0; Microsoft), or when appropriate (Fig. 1, D, H, and I; Fig. 2 B; Fig. 3 F; and Fig. 5, E and G) by a two-way ANOVA grouped test with subsequent Bonferroni posttest correction using Prism 5 software (GraphPad Software, Inc.).

Online supplemental material. Fig. S1 shows the accumulation of CD11b⁺Gr1⁺ MDSCs in liver and mesenteric lymph nodes after CLP. Fig. S2 shows a heat map with the complete list of genes shown in Fig. 4 A. Fig. S3 shows KC-induced chemotaxis of CD11b⁺Gr1⁺ cells isolated from spleen and bone marrow. Online supplemental material is available at http://www.jem.org/cgi/content/full/jem.20091474/DC1.

REFERENCES

Angus, D.C., W.T. Linde-Zwirble, J. Lidicker, G. Clermont, J. Carcillo, and M.R. Pinsky. 2001. Epidemiology of severe sepsis in the United States: analysis of incidence, outcome, and associated costs of care. Crit. Care Med. 29:1303–1310. doi:10.1097/00003246-200107000-00002

Badolato, R., J.M. Wang, W.J. Murphy, A.R. Lloyd, D.F. Michiel, L.L. Bausserman, D.J. Kelvin, and J.J. Oppenheim. 1994. Serum amyloid A is a chemoattractant: induction of migration, adhesion, and tissue infiltration of monocytes and polymorphonuclear leukocytes. J. Exp. Med. 180:203–209. doi:10.1084/jem.180.1.203

Bernard, G.R., J.L. Vincent, P.F. Laterre, S.P. LaRosa, J.F. Dhainaut, A. Lopez-Rodriguez, J.S. Steingrub, G.E. Garber, J.D. Helterbrand, E.W. Ely, and C.J. Fisher Jr.; Recombinant human protein C Worldwide Evaluation in Severe Sepsis (PROWESS) study group. 2001. Efficacy and safety of recombinant human activated protein C for severe sepsis. N. Engl. J. Med. 344:699–709. doi:10.1056/NEJM200103083441001

Betz, U.A., W. Bloch, M. van den Broek, K. Yoshida, T. Taga, T. Kishimoto, K. Addicks, K. Rajewsky, and W. Müller. 1998. Postnatally induced inactivation of gp130 in mice results in neurological, cardiac, hematopoietic, immunological, hepatic, and pulmonary defects. J. Exp. Med. 188:1955–1965. doi:10.1084/jem.188.10.1955

Bozic, C.R., L.F. Kolakowski Jr., N.P. Gerard, C. Garcia-Rodriguez, C. von Uexkull-Guldenband, M.J. Conklyn, R. Breslow, H.J. Showell, and C. Gerard. 1995. Expression and biologic characterization of the murine chemokine KC. J. Immunol. 154:6048–6057.

Buras, J.A., B. Holzmann, and M. Sitkovsky. 2005. Animal models of sepsis: setting the stage. Nat. Rev. Drug Discov. 4:854–865. doi:10.1038/nrd1854

Byl, B., I. Roucloux, A. Crusiaux, E. Dupont, and J. Devière. 1993. Tumor necrosis factor alpha and interleukin 6 plasma levels in infected cirrhotic patients. Gastroenterology. 104:1492–1497.

Cheng, N., R. He, J. Tian, P.P. Ye, and R.D. Ye. 2008a. Cutting edge: TLR2 is a functional receptor for acute-phase serum amyloid A. J. Immunol. 181:22–26.

Cheng, P., C.A. Corzo, N. Luetteke, B. Yu, S. Nagaraj, M.M. Bui, M. Ortiz, W. Nacken, C. Sorg, T. Vogl, et al. 2008b. Inhibition of dendritic cell differentiation and accumulation of myeloid-derived suppressor cells in cancer is regulated by S100A9 protein. J. Exp. Med. 205:2235–2249. doi:10.1084/jem.20080132

Christenson, K., L. Björkman, C. Tängemo, and J. Bylund. 2008. Serum amyloid A inhibits apoptosis of human neutrophils via a P2X7-sensitive pathway independent of formyl peptide receptor-like 1. J. Leukoc. Biol. 83:139–148. doi:10.1189/jlb.0507276

Delano, M.J., P.O. Scumpia, J.S. Weinstein, D. Coco, S. Nagaraj, K.M. Kelly-Scumpia, K.A. O'Malley, J.L. Wynn, S. Antonenko, S.Z. Al-Quran, et al. 2007. MyD88-dependent expansion of an immature GR-1+CD11b+ population induces T cell suppression and Th2 polarization in sepsis. J. Exp. Med. 204:1463–1474. doi:10.1084/jem.20062602

Ernst, M., M. Inglese, P. Waring, I.K. Campbell, S. Bao, F.J. Clay, W.S. Alexander, I.P. Wicks, D.M. Tarlinton, U. Novak, et al. 2001. Defective gp130-mediated signal transducer and activator of transcription (STAT) signaling results in degenerative joint disease, gastrointestinal ulceration, and failure of uterine implantation. J. Exp. Med. 194:189–203. doi:10.1084/jem.194.2.189

Fisher, C.J., Jr., J.M. Agosti, S.M. Opal, S.F. Lowry, R.A. Balk, J.C. Sadoff, E. Abraham, R.M. Schein, and E. Benjamin; The Soluble TNF Receptor Sepsis Study Group. 1996. Treatment of septic shock with the tumor necrosis factor receptor:Fc fusion protein. N. Engl. J. Med. 334:1697–1702. doi:10.1056/NEJM199606273342603

Foreman, M.G., D.M. Mannino, and M. Moss. 2003. Cirrhosis as a risk factor for sepsis and death: analysis of the National Hospital Discharge Survey. Chest. 124:1016–1020. doi:10.1378/chest.124.3.1016

Gabay, C., and I. Kushner. 1999. Acute-phase proteins and other systemic responses to inflammation. N. Engl. J. Med. 340:448–454. doi:10.1056/NEJM199902113400607

Gabrilovich, D.I., and S. Nagaraj. 2009. Myeloid-derived suppressor cells as regulators of the immune system. Nat. Rev. Immunol. 9:162–174. doi:10.1038/nri2506

Haile, L.A., R. von Wasielewski, J. Gamrekelashvili, C. Kruger, O. Bachmann, A.M. Westendorf, J. Buer, R. Liblau, M.P. Manns, F. Korangy, and T.F. Greten. 2008. Myeloid-derived suppressor cells in inflammatory bowel disease: a new immunoregulatory pathway. Gastroenterology. 135:871–881.

Hoechst, B., L.A. Ormandy, M. Ballmaier, F. Lehner, C. Krüger, M.P. Manns, T.F. Greten, and F. Korangy. 2008. A new population of myeloid-derived suppressor cells in hepatocellular carcinoma patients induces CD4(+)CD25(+)Foxp3(+) T cells. Gastroenterology. 135:234–243. doi:10.1053/j.gastro.2008.03.020

Hotchkiss, R.S., and I.E. Karl. 2003. The pathophysiology and treatment of sepsis. N. Engl. J. Med. 348:138–150. doi:10.1056/NEJMra021333

Hotchkiss, R.S., and D.W. Nicholson. 2006. Apoptosis and caspases regulate death and inflammation in sepsis. Nat. Rev. Immunol. 6:813–822. doi:10.1038/nri1943

Kim, K.D., J. Zhao, S. Auh, X. Yang, P. Du, H. Tang, and Y.X. Fu. 2007. Adaptive immune cells temper initial innate responses. Nat. Med. 13:1248–1252.

Klein, C., T. Wüstefeld, U. Assmus, T. Roskams, S. Rose-John, M. Müller, M.P. Manns, M. Ernst, and C. Trautwein. 2005. The IL-6-gp130-STAT3 pathway in hepatocytes triggers liver protection in T cell-mediated liver injury. J. Clin. Invest. 115:860–869.

Kopf, M., H. Baumann, G. Freer, M. Freudenberg, M. Lamers, T. Kishimoto, R. Zinkernagel, H. Bluethmann, and G. Köhler. 1994. Impaired immune and acute-phase responses in interleukin-6-deficient mice. Nature. 368:339–342. doi:10.1038/368339a0

Luchtefeld, M., H. Schunkert, M. Stoll, T. Selle, R. Lorier, K. Grote, C. Sagebiel, K. Jagavelu, U.J. Tietge, U. Assmus, et al. 2007. Signal transducer of inflammation gp130 modulates atherosclerosis in mice and man. J. Exp. Med. 204:1935–1944. doi:10.1084/jem.20070120

Matuschak, G.M. 1996. Lung-liver interactions in sepsis and multiple organ failure syndrome. Clin. Chest Med. 17:83–98. doi:10.1016/S0272-5231(05)70300-2

Medzhitov, R. 2007. Recognition of microorganisms and activation of the immune response. Nature. 449:819–826. doi:10.1038/nature06246

Movahedi, K., M. Guilliams, J. Van den Bossche, R. Van den Bergh, C. Gysemans, A. Beschin, P. De Baetselier, and J.A. Van Ginderachter. 2008. Identification of discrete tumor-induced myeloid-derived suppressor cell subpopulations with distinct T cell-suppressive activity. Blood. 111:4233–4244. doi:10.1182/blood-2007-07-099226

Murakami, M., M. Hibi, N. Nakagawa, T. Nakagawa, K. Yasukawa, K. Yamanishi, T. Taga, and T. Kishimoto. 1993. IL-6-induced homodimerization of gp130 and associated activation of a tyrosine kinase. Science. 260:1808–1810. doi:10.1126/science.8511589

Nagaraj, S., K. Gupta, V. Pisarev, L. Kinarsky, S. Sherman, L. Kang, D.L. Herber, J. Schneck, and D.I. Gabrilovich. 2007. Altered recognition of antigen is a mechanism of CD8+ T cell tolerance in cancer. Nat. Med. 13:828–835. doi:10.1038/nm1609

Nefedova, Y., M. Huang, S. Kusmartsev, R. Bhattacharya, P. Cheng, R. Salup, R. Jove, and D. Gabrilovich. 2004. Hyperactivation of STAT3 is involved in abnormal differentiation of dendritic cells in cancer. J. Immunol. 172:464–474.

Parrish, W.R., M. Gallowitsch-Puerta, C.J. Czura, and K.J. Tracey. 2008. Experimental therapeutic strategies for severe sepsis: mediators and mechanisms. *Ann. NY Acad. Sci.* 1144:210–236. doi:10.1196/annals.1418.011

Rebouissou, S., M. Amessou, G. Couchy, K. Poussin, S. Imbeaud, C. Pilati, T. Izard, C. Balabaud, P. Bioulac-Sage, and J. Zucman-Rossi. 2009. Frequent in-frame somatic deletions activate gp130 in inflammatory hepatocellular tumours. *Nature.* 457:200–204. doi:10.1038/nature07475

Riedemann, N.C., R.F. Guo, and P.A. Ward. 2003. Novel strategies for the treatment of sepsis. *Nat. Med.* 9:517–524. doi:10.1038/nm0503-517

Ritchie, D.G., and G.M. Fuller. 1983. Hepatocyte-stimulating factor: a monocyte-derived acute-phase regulatory protein. *Ann. NY Acad. Sci.* 408:490–502. doi:10.1111/j.1749-6632.1983.tb23268.x

Rittirsch, D., M.A. Flierl, and P.A. Ward. 2008. Harmful molecular mechanisms in sepsis. *Nat. Rev. Immunol.* 8:776–787. doi:10.1038/nri2402

Rittirsch, D., M.S. Huber-Lang, M.A. Flierl, and P.A. Ward. 2009. Immunodesign of experimental sepsis by cecal ligation and puncture. *Nat. Protoc.* 4:31–36. doi:10.1038/nprot.2008.214

Shah, C., R. Hari-Dass, and J.G. Raynes. 2006. Serum amyloid A is an innate immune opsonin for Gram-negative bacteria. *Blood.* 108:1751–1757. doi:10.1182/blood-2005-11-011932

Sinha, P., V.K. Clements, S.K. Bunt, S.M. Albelda, and S. Ostrand-Rosenberg. 2007. Cross-talk between myeloid-derived suppressor cells and macrophages subverts tumor immunity toward a type 2 response. *J. Immunol.* 179:977–983.

Streetz, K.L., T. Wüstefeld, C. Klein, K.J. Kallen, F. Tronche, U.A. Betz, G. Schütz, M.P. Manns, W. Müller, and C. Trautwein. 2003. Lack of gp130 expression in hepatocytes promotes liver injury. *Gastroenterology.* 125:532–543. doi:10.1016/S0016-5085(03)00901-6

Tebbutt, N.C., A.S. Giraud, M. Inglese, B. Jenkins, P. Waring, F.J. Clay, S. Malki, B.M. Alderman, D. Grail, F. Hollande, et al. 2002. Reciprocal regulation of gastrointestinal homeostasis by SHP2 and STAT-mediated trefoil gene activation in gp130 mutant mice. *Nat. Med.* 8:1089–1097. doi:10.1038/nm763

Wuestefeld, T., C. Klein, K.L. Streetz, U. Betz, J. Lauber, J. Buer, M.P. Manns, W. Müller, and C. Trautwein. 2003. Interleukin-6/glycoprotein 130-dependent pathways are protective during liver regeneration. *J. Biol. Chem.* 278:11281–11288. doi:10.1074/jbc.M208470200

Yang, L., J. Huang, X. Ren, A.E. Gorska, A. Chytil, M. Aakre, D.P. Carbone, L.M. Matrisian, A. Richmond, P.C. Lin, and H.L. Moses. 2008. Abrogation of TGF beta signaling in mammary carcinomas recruits Gr-1+CD11b+ myeloid cells that promote metastasis. *Cancer Cell.* 13:23–35. doi:10.1016/j.ccr.2007.12.004

Young, M.R., M. Newby, and H.T. Wepsic. 1987. Hematopoiesis and suppressor bone marrow cells in mice bearing large metastatic Lewis lung carcinoma tumors. *Cancer Res.* 47:100–105.

Zhu, B., Y. Bando, S. Xiao, K. Yang, A.C. Anderson, V.K. Kuchroo, and S.J. Khoury. 2007. CD11b+Ly-6C(hi) suppressive monocytes in experimental autoimmune encephalomyelitis. *J. Immunol.* 179:5228–5237.

Zouki, C., M. Beauchamp, C. Baron, and J.G. Filep. 1997. Prevention of In vitro neutrophil adhesion to endothelial cells through shedding of L-selectin by C-reactive protein and peptides derived from C-reactive protein. *J. Clin. Invest.* 100:522–529. doi:10.1172/JCI119561

Acute-phase proteins mobilize MDSCs | Sander et al.